

Semiautomatic three-dimensional CT ventricular volumetry in patients with congenital heart disease: agreement between two methods with different user interaction

Hyun Woo Goo¹ · Sang-Hyub Park¹

Received: 17 August 2015 / Accepted: 20 August 2015 / Published online: 29 August 2015
© Springer Science+Business Media Dordrecht 2015

Abstract To assess agreement between two semi-automatic, three-dimensional (3D) computed tomography (CT) ventricular volumetry methods with different user interactions in patients with congenital heart disease. In 30 patients with congenital heart disease (median age 8 years, range 5 days–33 years; 20 men), dual-source, multi-section, electrocardiography-synchronized cardiac CT was obtained at the end-systolic ($n = 22$) and/or end-diastolic ($n = 28$) phase. Nineteen left ventricle end-systolic (LV ESV), 28 left ventricle end-diastolic (LV EDV), 22 right ventricle end-systolic (RV ESV), and 28 right ventricle end-diastolic volumes (RV EDV) were successfully calculated using two semi-automatic, 3D segmentation methods with different user interactions (high in method 1, low in method 2). The calculated ventricular volumes of the two methods were compared and correlated. A P value <0.05 was considered statistically significant. LV ESV (35.95 ± 23.49 ml), LV EDV (88.76 ± 61.83 ml), and RV ESV (46.87 ± 47.39 ml) measured by method 2 were slightly but significantly smaller than those measured by method 1 (41.25 ± 26.94 ml, 92.20 ± 62.69 ml, 53.61 ± 50.08 ml for LV ESV, LV EDV, and RV ESV, respectively; $P \leq 0.02$). In contrast, no statistically significant difference in RV EDV (122.57 ± 88.57 ml in method 1, 123.83 ± 89.89 ml in method 2; $P = 0.36$) was found between the two methods. All ventricular volumes showed very high correlation ($R = 0.978, 0.993, 0.985, 0.997$ for

LV ESV, LV EDV, RV ESV, and RV EDV, respectively; $P < 0.001$) between the two methods. In patients with congenital heart disease, 3D CT ventricular volumetry shows good agreement and high correlation between the two methods, but method 2 tends to slightly underestimate LV ESV, LV EDV, and RV ESV.

Keywords Multi-detector row CT · Comparative study · Ventricular volumetry · Congenital heart disease · Cardiac CT

Introduction

Ventricular volume measurement is of critical importance in patients with congenital heart disease (CHD) because it provides an assessment of global ventricular function essential for determining treatment planning and predicting clinical outcome. Imaging modalities used for this measurement include echocardiography, cardiac magnetic resonance imaging (MRI), and cardiac computed tomography (CT). Echocardiographic measurement is limited by geometric assumptions and incomplete imaging windows. Cardiac MRI is currently regarded as the reference standard of this measurement. Cardiac CT using state-of-the-art imaging techniques has recently been used for ventricular volumetry and is suggested as an alternative imaging modality to cardiac MRI, offering more accurate values and easier postprocessing mainly due to better image quality [1–3].

Various segmentation methods have been used for ventricular volumetry [4]. The two-dimensional (2D) simplified endocardial contouring and disc summation method is most commonly used and is regarded as the current standard. However, this method is time-consuming

✉ Hyun Woo Goo
hwgoo@amc.seoul.kr

¹ Department of Radiology and Research Institute of Radiology, Asan Medical Center, University of Ulsan College of Medicine, 88, Olympic-ro 43-gil, Songpa-gu, Seoul, Republic of Korea

and subject to substantial inter-reader variability ($\sim 8\%$ for the left ventricle [LV], $\sim 22\%$ for the right ventricle [RV]) and various sources of error due to valvular levels, papillary muscles/trabeculations, inconsistent breath-holding, and the Simpson method. Consequently, a three-dimensional (3D) or volumetric segmentation method is highly recommended in order to achieve high accuracy and reproducibility of ventricular volumetry [5–8]. Such segmentation methods often use different levels of user interaction. User interaction is not necessary for fully automated software, while various degrees of user adjustment are required for a semi-automatic segmentation method. The effect of user interaction on accuracy of 3D, semi-automatic ventricular volumetry has rarely been investigated, particularly using cardiac CT data.

Therefore, this study was performed to assess agreement between two semi-automatic, 3D CT ventricular volumetry methods with different user interactions in patients with CHD.

Materials and methods

This retrospective study was approved by the Institutional Review Board of our hospital, which waived informed consent.

In 30 patients with CHD (median age 8 years, range 5 days–33 years; 20 males), dual-source, multi-section, electrocardiography (ECG)-synchronized cardiac CT (Somatom Definition FLASH; Siemens Healthcare, Forchheim, Germany) was performed. CHDs included in the study population were tetralogy of Fallot in 14 patients, double outlet RV in two, pulmonary atresia with ventricular septal defect in two, aortic stenosis in two, and others in the remaining 10. None of the patients had metallic implants or wires that might cause artifacts on cardiac CT images. Retrospective ECG-gated spiral scanning was used in 20 patients, and prospective ECG-triggered sequential scanning was used in 10 patients. Of the 10 patients who underwent prospective ECG-triggered scanning, additional respiratory triggering was used to reduce respiratory motion artifacts in seven free-breathing young children [3]. End-systolic and end-diastolic phases were selected visually by previewing multiple cardiac phases or automatically using a motion map [9]. Both end-systolic and end-diastolic phases were obtained in 20 patients, end-diastolic phase alone in eight, and end-systolic phase alone in two. Therefore, 22 end-systolic and 28 end-diastolic phases were acquired in 30 patients. Scanning parameters were 64×0.6 mm detector collimation, 128 slices using the z-flying focal spot technology, 0.28-s gantry rotation time, 75-ms temporal resolution, 0.75-mm slice thickness, and 0.4-mm reconstruction interval. ECG-controlled tube

current modulation was used for retrospective ECG-gated spiral scanning, and combined tube current modulation (CARE Dose 4D; Siemens Healthcare) was used in all cases. A sinogram-affirmed iterative reconstruction algorithm (SAFIRE, strength of 5; Siemens Healthcare) rather than the conventional filtered back projection algorithm was used for image reconstruction. CT radiation dose was individually determined on the basis of the measured cross-sectional area and body density of each patient [10]. One hundred kV was used for retrospective ECG-gated spiral scanning except for one case with 120 kV, while 80 kV was used for prospective ECG-triggered sequential scanning. The volume CT dose index (mGy) and dose-length product (mGy cm) values were 17.5 ± 6.7 and 497.8 ± 197.7 , respectively, for retrospective ECG-gated spiral scanning and 1.4 ± 0.1 and 15.8 ± 6.2 , respectively, for prospective ECG-triggered sequential scanning. The radiation dose of cardiac CT was estimated based on the International Commission on Radiological Protection (ICRP) publication 103 [11]. The calculated effective dose (mSv) was 7.4 ± 3.4 for retrospective ECG-gated spiral scanning and 0.9 ± 0.3 for prospective ECG-triggered sequential scanning.

Iodinated contrast agent (Iomeron 400, 400 mg I/ml; Bracco Imaging SpA, Milan, Italy; 1.5–2.0 ml/kg) was intravenously administered with a dual-head power injector at an injection rate of 0.3–3.0 ml/s via the arm or leg vein. A triphasic injection protocol (undiluted \rightarrow 50 % diluted \rightarrow 5 % diluted) was used to achieve uniform opacification of cardiovascular structures, including the RV, and to avoid perivenous streak artifacts caused by undiluted contrast agent [12]. The scan delay time of cardiac CT was determined using a bolus tracking technique in which a region of interest was placed in the left ventricular cavity with a trigger threshold of 150 Hounsfield units (HU). Scanning started without breathing instruction 5 s after bolus detection in young children or with breath-holding instruction 8 s after bolus detection in cooperative patients. To ensure sufficient contrast enhancement in the LV and RV cavities in order to allow 3D threshold-based segmentation, CT attenuation was measured in the LV cavity, the RV cavity, and the interventricular septum by placing a rectangular regions of interest. The measured CT attenuation values of the LV and RV cavities were compared.

LV end-systolic volume (ESV), LV end-diastolic volume (EDV), RV ESV, and RV EDV were calculated with two different commercially available methods using a semi-automatic 3D segmentation but a different user interaction (Table 1). Method 1 utilized a commercially available workstation (Advantage Windows 4.6; GE Healthcare, Milwaukee, WI, USA) with 3D threshold-based, region-growing segmentation necessitating

Table 1 Comparison of two semi-automatic, three-dimensional segmentation methods

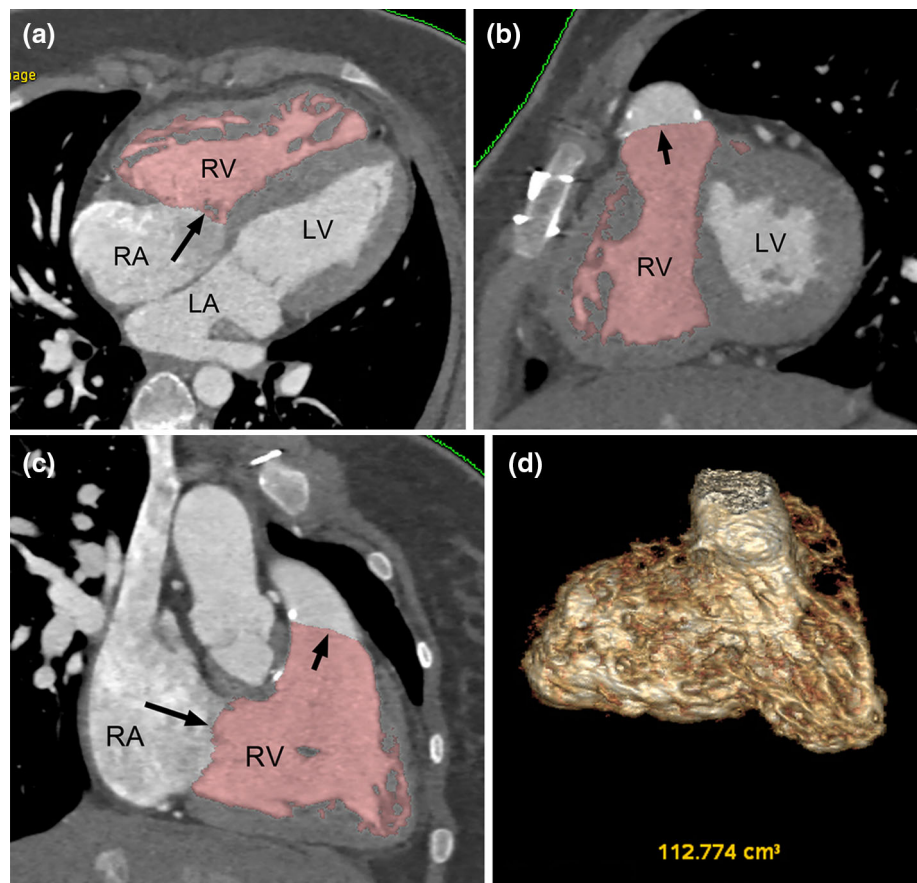
	Method 1	Method 2
Basic logic for segmentation	Threshold-based	Threshold- and shape-based
Detailed endocardial contour	Semi-automatic detection	Automatic detection by mouse clicks, not adjustable
Cardiac valve planes	Three-dimensional manual segmentation	Automatic detection by mouse clicks, not adjustable
Typical postprocessing time	Longer (10–15 min)	Shorter (\leq several min)

higher user interaction (Fig. 1). In this method, detailed endocardial contours were created using a threshold-based segmentation approach in which an optimal threshold for each cardiac phase was manually selected from the interventricular septum and adjacent ventricular cavities assisted by a histogram-based analysis [13]. As a result, the papillary muscles and trabeculations were excluded from ventricular volumes. The atrioventricular valve planes were manually adjusted using 3D region-growing editing, and the semilunar valve planes or ventricular septal defects (if present) were manually corrected using volume cutting. Another commercially available workstation (syngo InSpace EP; Siemens Healthcare) with 3D threshold- and shape-based segmentation requiring lower user interaction, i.e., one or several mouse-clicks, was used in method 2 (Fig. 2).

Detailed endocardial contours and the valve planes were automatically determined in method 2. In contrast to method 1, user input was necessary only for identifying a ventricular cavity, and manual editing was not permitted in method 2. These two segmentation methods were performed independently, blinded to results of the other method.

All statistical analyses were performed using SPSS statistical software version 20.0 (IBM, Chicago, IL, USA). The calculated ventricular volumes of the two methods were compared and correlated. Paired *t* test and Pearson correlation were used for these analyses. Moreover, intra-class correlation coefficient (ICC) and Bland–Altman plot were used to demonstrate the agreement between the two methods. A *P* value <0.05 was considered statistically significant.

Fig. 1 Three-dimensional CT right ventricular volumetry using method 1 in a 12-year-old girl with double outlet right ventricle and remote ventricular septal defect who underwent Rastelli operation. Four-chamber (a), short-axis (b), and right ventricular long-axis (c) CT images show segmented right ventricular cavity in pink. Potential sources of error in right ventricular volumetry were minimized at the papillary muscles, the trabeculations, and the tricuspid (*long arrow*) and pulmonary (*short arrow*) valve planes using a three-dimensional, threshold-based segmentation approach with high user interaction (method 1). The calculated right ventricular end-systolic volume was approximately 113 ml (d). LA left atrium, LV left ventricle, RA right atrium, RV right ventricle



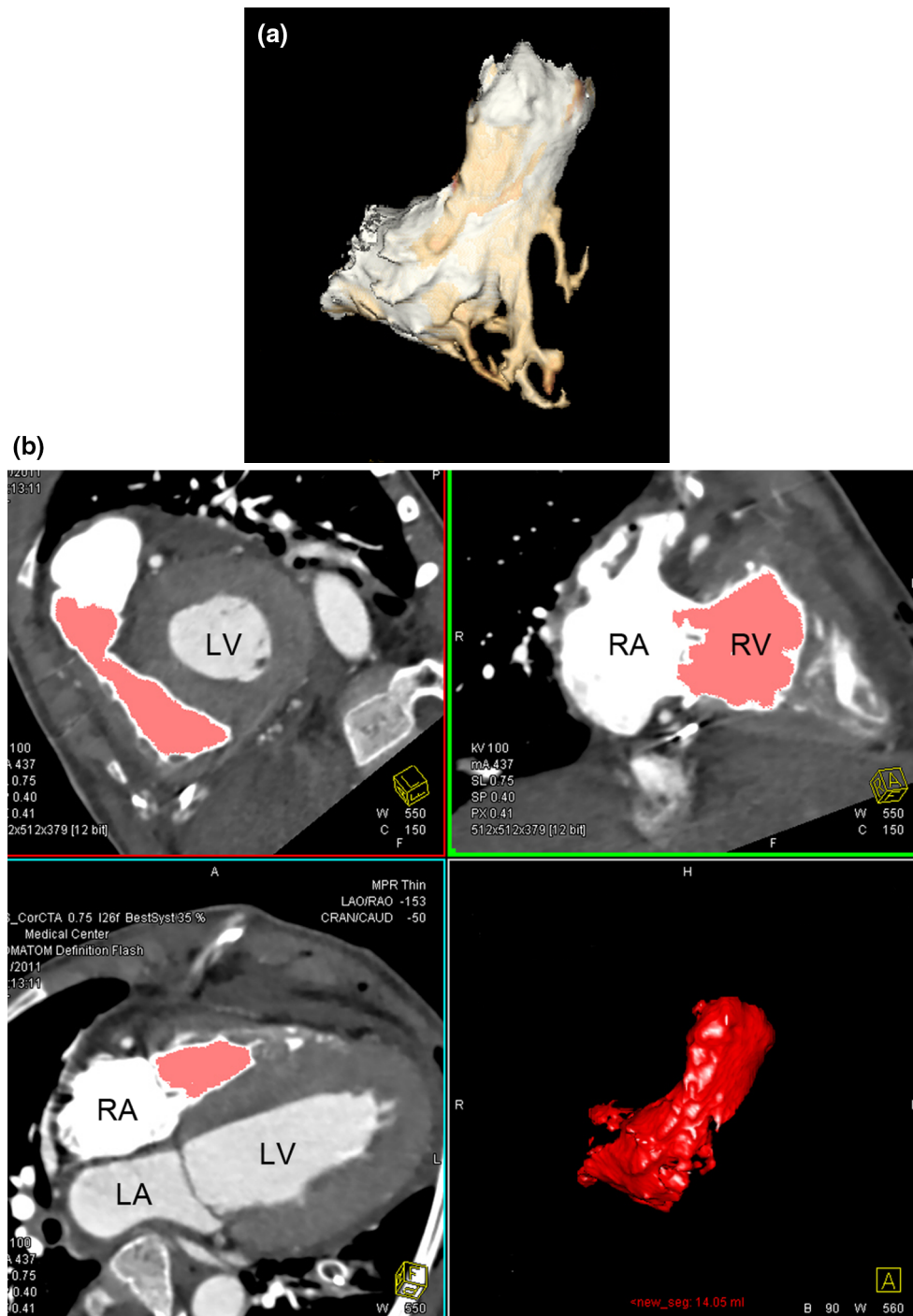


Fig. 2 Three-dimensional right ventricular volumetry in an 8-year-old boy with aortic stenosis. Compared with the right ventricular end-systolic volume segmented by method 1 (a), peripheral rims of the right ventricle are not included in the right ventricular cavity in

method 2 (b), which results in underestimation of the calculated right ventricular volume. *LA* left atrium, *LV* left ventricle, *RA* right atrium, *RV* right ventricle

Results

All 30 patients completed dual-source, multi-section, ECG-synchronized cardiac CT without complications. The measured CT attenuation values in the LV cavity, the RV

cavity, and the interventricular septum were 369.28 ± 67.98 HU, 375.31 ± 103.54 HU, and 104.78 ± 19.17 HU, respectively. No significant difference in measured CT attenuation values was found between the LV and RV cavities ($P > 0.05$).

Method 2 could not segment LV ESV in three patients due to incorrect identification of the LV cavity or extensive leakage to other regions. Nineteen LV ESVs, 28 LV EDVs, 22 RV ESVs, and 28 RV EDVs were successfully calculated using both methods and eventually included in the comparative analysis of this study. LV ESV (35.95 ± 23.49 ml), LV EDV (88.76 ± 61.83 ml), and RV ESV (46.87 ± 47.39 ml) measured by method 2 were slightly but significantly smaller than those measured by method 1 (41.25 ± 26.94 ml, 92.20 ± 62.69 ml, 53.61 ± 50.08 ml for LV ESV, LV EDV, and RV ESV, respectively; $P \leq 0.02$) (Table 2). In the majority of these cases, method 2 was limited in performing detailed segmentation including peripheral ventricular portions adjacent to the ventricular walls or the valves into a whole ventricular cavity (Fig. 2). In contrast, no statistically significant difference in RV EDV (122.57 ± 88.57 ml in method 1, 123.83 ± 89.89 ml in method 2; $P = 0.36$) was found between the two methods (Table 2). All the ventricular volumes showed very high correlation ($R = 0.978, 0.993, 0.985, 0.997$ for LV ESV, LV EDV, RV ESV, and RV EDV, respectively; $P < 0.001$) between the two methods (Table 2) (Figs. 3, 4). ICC results for inter-method agreement were greater than 0.9 for all measured ventricular volumes, indicating excellent inter-method agreement (Table 3). The Bland–Altman plots also demonstrated good agreement between the two methods, with the upper 95 % limit of agreement ranging from 12.8 to 24.3 ml and the lower 95 % limit of agreement ranging from -7.1 to -15.3 ml (Fig. 5). If a percentage difference rather than an absolute difference was used for the y-axis of the Bland–Altman plot (not shown), the 95 % limits of agreement were greater for LV ESV (54.0, -18.5 %) and RV ESV (63.5, -21.4 %) than for LV EDV (22.2, -10.9 %) and RV EDV (15.3, -13.1 %).

Discussion

This study demonstrated that 3D CT ventricular volumetry in patients with CHD was technically feasible using two commercially available software packages: method 1, threshold-based endocardial segmentation and manual

segmentation of valve planes, and method 2, threshold- and shape-based near-automatic segmentation not allowing manual adjustment. In this study, 3D CT ventricular volumetry shows good agreement and high correlation between the two methods in patients with CHD, but method 2 tends to slightly underestimate LV ESV, LV EDV, and RV ESV. Therefore, method 1 seems to be preferred in order to obtain accurate ventricular volumes at the expense of more user interactions and longer postprocessing time.

Accurate and reproducible determination of LV and RV volumes is of critical importance for clinical diagnosis, treatment planning, and prognostic prediction in patients with CHD. Currently, a simplified endocardial contouring method using 2D short-axis or, less frequently, axial cine MRI is regarded as the reference standard. However, the method is limited by considerable errors resulting from inclusion of the papillary muscles and trabeculations as part of the ventricular volume and inaccurate determination of the atrioventricular and semilunar valve planes [1, 4, 14–17]. The former error results in overestimation of ventricular volumes and underestimation of ejection fraction (EF) and ventricular mass. These inaccuracies can be overcome through the use of a detailed but time-consuming manual endocardial contouring method or a threshold-based segmentation method. The latter error may be reduced through cross-referenced identification of the valve planes using long-axis cine MRI [16]. In addition, the simplified endocardial contouring method is subject to intra- or interobserver variability that cannot be ignored, particularly for the complex anatomy of the RV. In a study using cross-referencing evaluated by expert observers [18], the variabilities of indexed RV EDV and RV EF were non-negligible, up to 20 ml/m² and 3.0 EF %. Beerbaum et al. [19] demonstrated that consensus training reduced inter-institutional variance in cardiac function measured by MRI in patients with CHD.

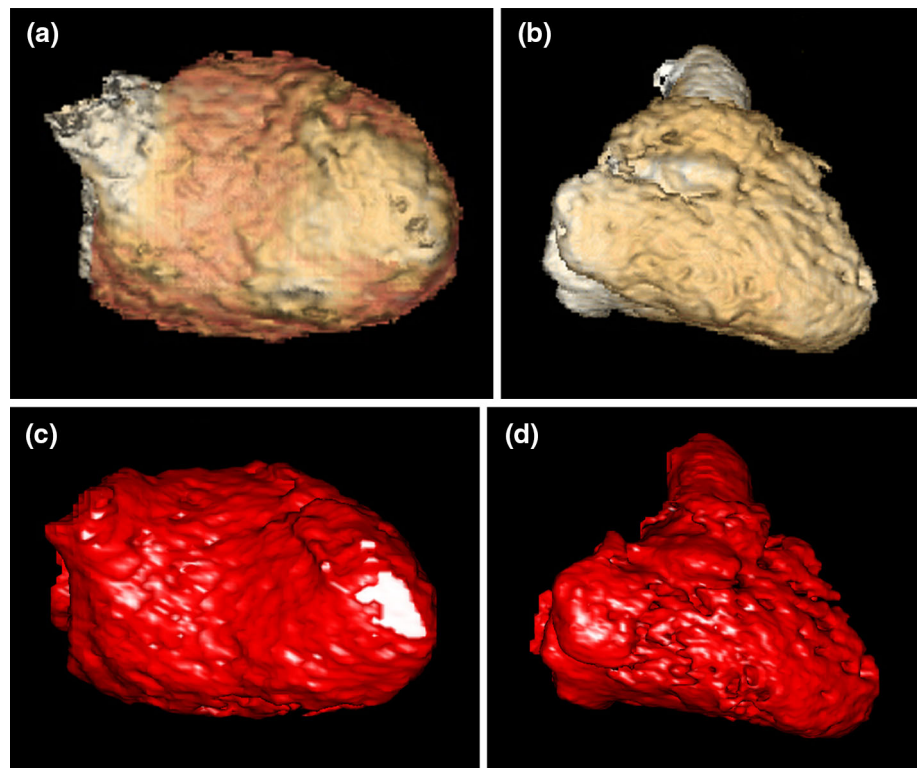
Most previous studies have used 2D disc summation for ventricular volumetry irrespective of either an endocardial contouring or threshold-based segmentation method. An in vitro comparative MRI study using static RV-shaped phantoms showed that 3D analysis (<1 % error) was more accurate than a 2D disc summation method (~ 20 % error)

Table 2 Comparison and correlation of ventricular volumes measured by two three-dimensional segmentation methods

	Method 1	Method 2	Difference between two methods	95 % Confidence interval	<i>P</i> value	Pearson correlation coefficient (<i>R</i>)	<i>P</i> value
LV ESV (ml, <i>n</i> = 19)	41.25 ± 26.94	35.95 ± 23.49	5.30 ± 6.33	2.25, 8.35	0.002	0.978	<0.001
LV EDV (ml, <i>n</i> = 28)	92.20 ± 62.69	88.76 ± 61.83	3.44 ± 7.33	0.59, 6.28	0.02	0.993	<0.001
RV ESV (ml, <i>n</i> = 22)	53.61 ± 50.08	46.87 ± 47.39	6.74 ± 8.98	2.76, 10.72	0.002	0.985	<0.001
RV EDV (ml, <i>n</i> = 28)	122.57 ± 88.57	123.83 ± 89.89	-1.26 ± 7.16	$-4.04, 1.51$	0.36	0.997	<0.001

EDV end-diastolic volume, ESV end-systolic volume, LV left ventricular, RV right ventricular

Fig. 3 Three-dimensional CT ventricular volumetry in an 8-month-old girl with repaired tetralogy of Fallot. Left ventricle and right ventricle end-diastolic volumes (26.1 and 19.9 ml, respectively) calculated by method 1 (**a**, **b**) were comparable to those (20.9 and 19.5 ml, respectively) calculated by method 2 (**c**, **d**)



[20]. Consequently, a 3D threshold-based segmentation method is recommended to achieve highly accurate and reproducible results of ventricular volumetry with high time-efficiency [5–8]. Unfortunately, we found that commercial software providing a 3D threshold-based segmentation approach is barely available, particularly for RV volume measurements. We tested two 3D threshold-based segmentation methods available for both LV and RV volumetry in this study. The two methods are semi-automatic, but different levels of user inputs are required for ventricular volumetry. Ideally, lower levels of user interactions are preferred at the same accuracy. As found in this study, certain levels of user interactions are still necessary to achieve highly accurate LV and RV volumes in patients with CHD. In other words, commercially available semi- or automatic software packages are commonly imperfect, particularly in patients with complex cardiac morphology.

In this study, 3D cardiac CT data were used for ventricular volumetry rather than 2D cardiac MRI data in order to take advantage of a 3D threshold-based segmentation approach. 3D cardiac CT data were frequently downgraded to reformatted 2D data in previous studies [1, 6–8, 21–23]. Compared with MRI ventricular volumetry, CT ventricular volumetry tends to overestimate ventricular volumes [20, 23]. This overestimation by CT has been assumed to be due, at least in part, to limited temporal resolution of cardiac CT, but the exact cause of the overestimation remains to be fully clarified. It is noteworthy that the fidelity of a

threshold-based segmentation approach is critically affected by image quality of data used for the evaluation [5]. In this respect, cardiac MRI is apt to be affected by various artifacts caused by motion, blood flow, magnetic field inhomogeneity, and metallic implants [5], while low or inhomogeneous ventricular enhancement on cardiac CT, more frequent in the right ventricle, can compromise the accuracy of ventricular volumetry using 3D threshold-based segmentation [23]. Such suboptimal contrast enhancement of the RV is commonly encountered in a biphasic contrast injection protocol. In contrast, a triphasic contrast injection protocol [12] was shown to have a high success rate (100 %) with 3D threshold-based segmentation in this study. The mean differences in CT attenuation values between the ventricular cavities and the interventricular septum were 264 HU for the LV and 270 HU for the RV, respectively. These mean differences were greater than those (205–208 HU) previously regarded as being sufficient for 3D threshold-based segmentation [6]. Moreover, scan parameters optimized for body size and iterative reconstruction algorithm were used to achieve good image quality with low image noise in this study. Previous phantom studies [21, 22] found that a first-generation, dual-source CT scanner (83-ms temporal resolution) allowed reliable results of ventricular volumetry independent of heart rate, up to 140 bpm. In this study, a second-generation, dual-source CT scanner with a slightly higher temporal resolution (75 ms) was used.

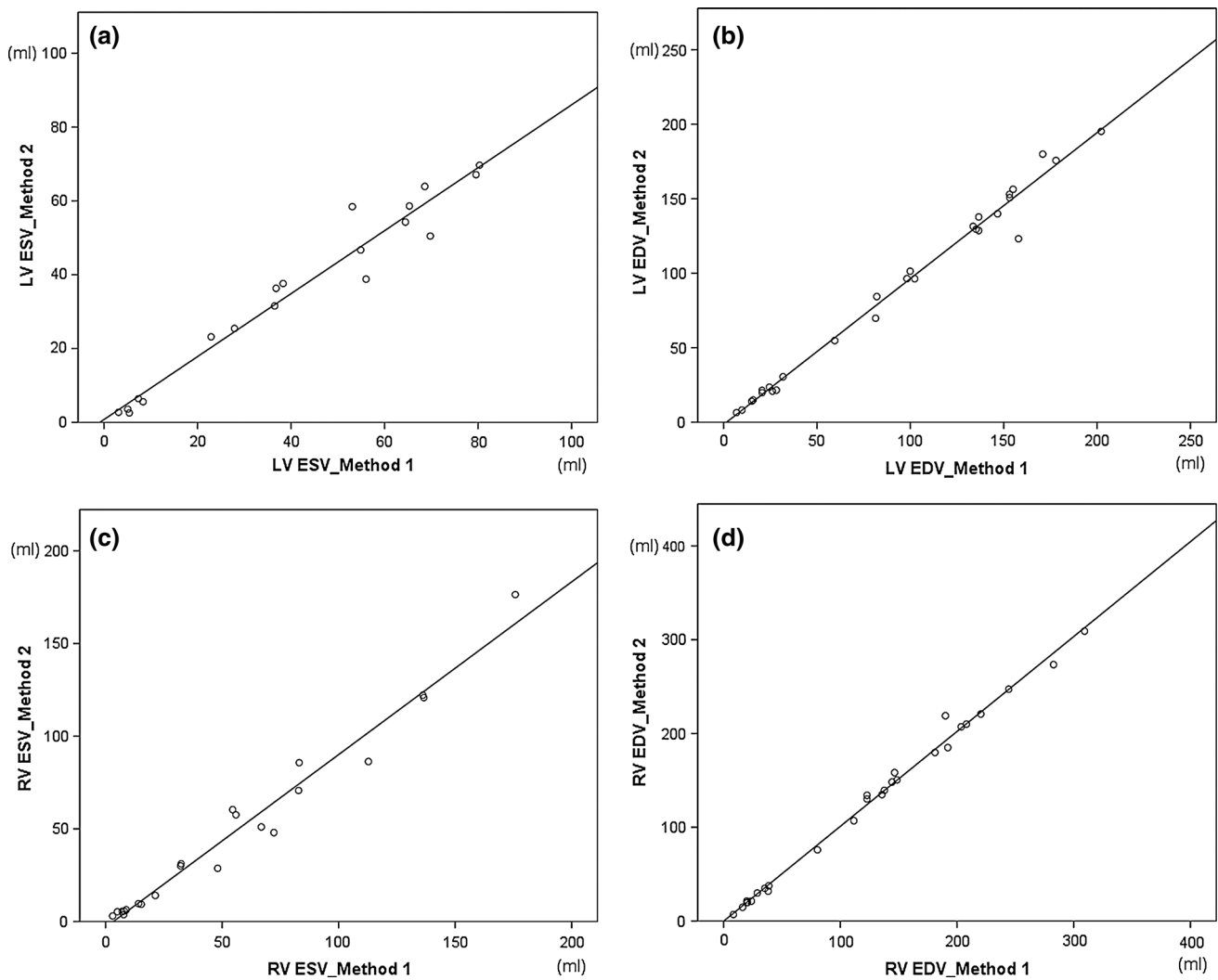


Fig. 4 Scatter diagrams show results of linear regression of ventricular volumes between the two semi-automatic, three-dimensional, threshold-based segmentation methods using cardiac CT data for left ventricular end-systolic volume (a), left ventricular end-diastolic

volume (b), right ventricular end-systolic volume (c), and right ventricular end-diastolic volume (d). EDV end-diastolic volume, ESV end-systolic volume, LV left ventricular, RV right ventricular

Table 3 Intraclass correlation coefficients (ICC) for inter-method agreement between the two three-dimensional CT ventricular volumetry methods

	Intraclass correlation coefficient (ICC)	P value
LV ESV (n = 19)	0.974	<0.001
LV EDV (n = 28)	0.996	<0.001
RV ESV (n = 22)	0.987	<0.001
RV EDV (n = 28)	0.998	<0.001

EDV end-diastolic volume, ESV end-systolic volume, LV left ventricular, RV right ventricular

There is need for a fast semi- or automatic 3D threshold-based segmentation approach requiring less or no user inputs while maintaining high accuracy and reliability even for complex cardiac morphology. Method 2 used in this study approaches this ideal method; however, it underestimates ventricular volumes particularly at the end-systolic phase (−12 % for LV ESV, −3 % for LV EDV, −13 %

for RV ESV) mainly because of lack of manual correction (Fig. 2). In addition, method 2 failed to segment LV ESV in three patients. A semi- or automatic-segmentation method is often problematic in cases of valve opening, ventricular septal defect, or other complex ventricular morphology, thereby necessitating manual corrections for accurate segmentation [1, 8]. On the contrary, the ability of

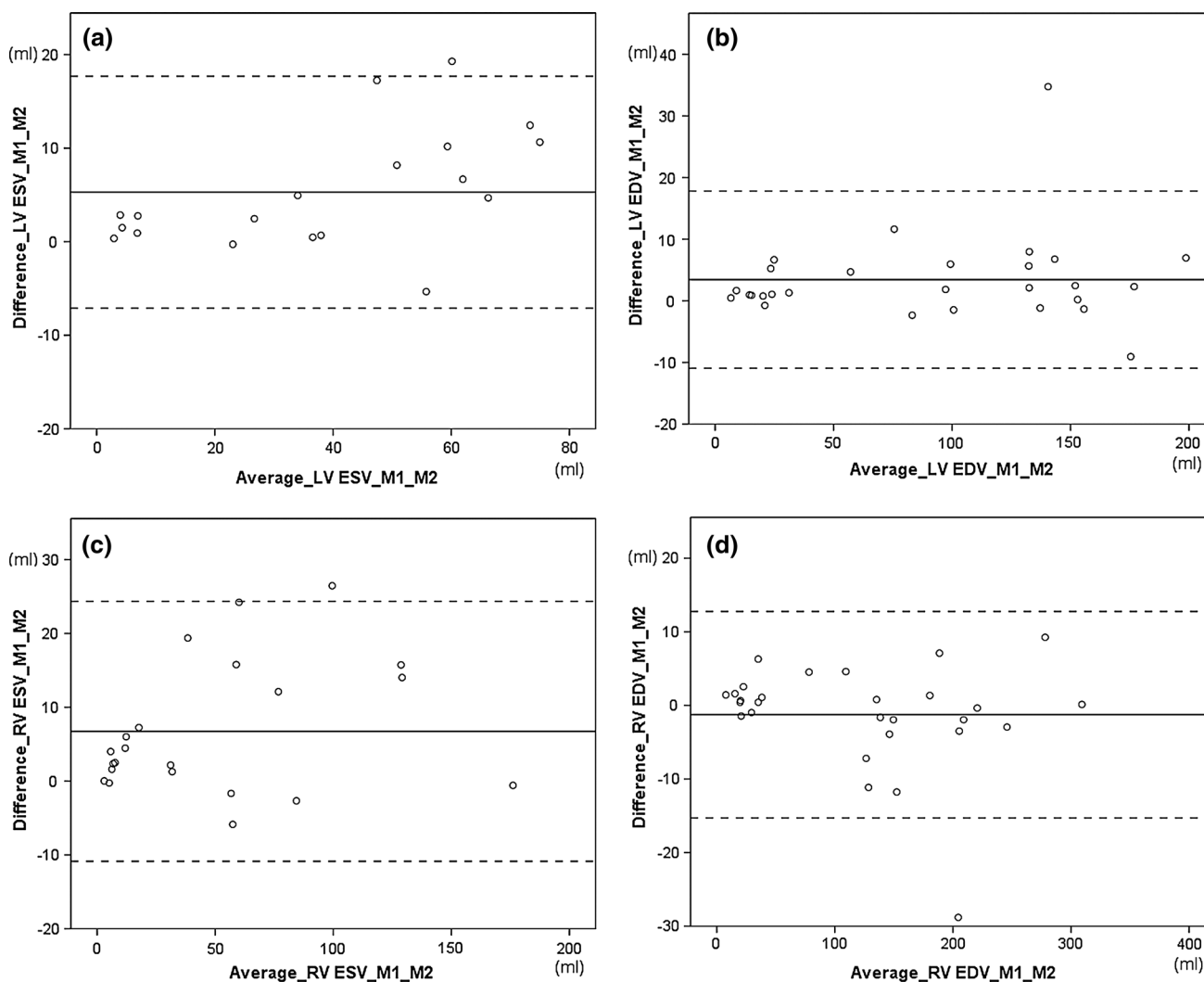


Fig. 5 Bland–Altman plots demonstrate limits of agreement of ventricular volumes between the two semi-automatic, three-dimensional, threshold-based segmentation methods using cardiac CT data for left ventricular end-systolic volume (a), left ventricular end-

diastolic volume (b), right ventricular end-systolic volume (c), and right ventricular end-diastolic volume (d). *EDV* end-diastolic volume, *ESV* end-systolic volume, *LV* left ventricular, *M1* method 1, *M2* method 2, *RV* right ventricular

manual correction in method 1 was invaluable in the achievement of a clinically acceptable level of accurately segmented LV and RV volumes in patients with CHD. A previous study also showed that manual adjustment was necessary for an automated LV segmentation method in approximately 40 % of the cases [24].

Method 1 used with 3D threshold-based, semi-automatic CT ventricular volumetry has great clinical implications due to its provision of accurate ventricular volumetry in patients with CHD, e.g., in determining optimal timing of pulmonary valve replacement in a dilated RV of repaired tetralogy of Fallot [17] and in determining bi- or uni-ventricular repair in a marginally small LV [25]. The approach also appears exceedingly useful for accurate functional evaluation in hypertrophic cardiomyopathy and myocardial

noncompaction in which a simplified endocardial contouring method offers misleading results [26, 27]. It should be noted that the current reference values from a simplified endocardial contouring method are not applicable for a 3D threshold-based segmentation method, as papillary muscles and trabeculations are handled differently, and new reference values need to be developed.

This study has several limitations. First, the number of patients evaluated in this study was relatively small. However, the main objective of this study was to assess agreement between two semi-automatic, 3D CT ventricular volumetry methods with different user interactions in patients with CHD, which was fairly accomplished with good statistical profiles. Thus, the inclusion of more patients may not drastically change the results of this study.

Second, the histogram-assisted strategy used to determine the optimal threshold in method 1 cannot perfectly eliminate partial volume averaging effects between ventricular blood and the myocardium. A partial voxel interpolation approach should be used to reduce this partial volume averaging effect, but no such software package is commercially available [24]. Nevertheless, the wide availability of method 1 is expected to produce notable progress in ventricular volumetry. Third, intra- and interobserver variabilities were not evaluated in this study because high reproducibility of a semi-automatic, 3D threshold-based segmentation method was already demonstrated in previous studies [1, 5]. Fourth, processing times were not compared between the two methods in this retrospective study because they were not individually recorded and they depend directly on the level of user interaction. According to our experiences, postprocessing time was approximately 10–15 min for each ventricular volume in method 1 and less than several minutes in method 2, depending on the number of user interactions. To improve clinical workflow, processing times for method 1 need to be shortened while maintaining high accuracy of ventricular volumetry.

In conclusion, 3D CT ventricular volumetry shows good agreement and high correlation between the two methods in patients with CHD, but method 2 tends to slightly underestimate LV ESV, LV EDV, and RV ESV. We decided to use method 1 in clinical practice due to the results of this study.

Compliance with ethical standards

Conflict of interest Hyun Woo Goo declares that he has no conflict of interest. Sang-Hyub Park declares that he has no conflict of interest.

Ethical approval All procedures performed in studies involving human participants were in accordance with the ethical standards of the institutional and/or national research committee and with the 1964 Helsinki declaration and its later amendments or comparable ethical standards.

Informed consent Informed consent was waived by our Institutional Review Board in the retrospective study.

References

- van Ooijen PM, de Jonge GJ, Oudkerk M (2012) Informatics in radiology: postprocessing pitfalls in using CT for automatic and semiautomatic determination of global left ventricular function. *Radiographics* 32(2):589–599
- Goo HW (2010) State-of-the-art CT imaging techniques for congenital heart disease. *Korean J Radiol* 11(1):4–18
- Goo HW (2011) Cardiac MDCT in children: CT technology overview and interpretation. *Radiol Clin North Am* 49(5):997–1010
- Petitjean C, Dacher JN (2011) A review of segmentation methods in short axis cardiac MR images. *Med Image Anal* 15(2):169–184
- Nassenstein K, de Greiff A, Hunold P (2009) MR evaluation of left ventricular volumes and function: threshold-based 3D segmentation versus short-axis planimetry. *Invest Radiol* 44(10):635–640
- Juergens KU, Seifarth H, Range F, Wienbeck S, Wenker M, Heindel W, Fischbach R (2008) Automated threshold-based 3D segmentation versus short-axis planimetry for assessment of global left ventricular function with dual-source MDCT. *AJR Am J Roentgenol* 190(2):308–314
- de Jonge GJ, van der Vleuten PA, Overbosch J, Lubbers DD, Jansen-van der Weide MC, Zijlstra F, van Ooijen PM, Oudkerk M (2011) Semi-automatic measurement of left ventricular function on dual source computed tomography using five different software tools in comparison with magnetic resonance imaging. *Eur J Radiol* 80(3):755–766
- de Jonge GJ, van Ooijen PM, Overbosch J, Gueorguieva AL, Janssen-van der Weide MC, Oudkerk M (2011) Comparison of (semi-)automatic and manually adjusted measurements of left ventricular function in dual source computed tomography using three different software tools. *Int J Cardiovasc Imaging* 27(6):787–794
- Ruzsics B, Gebregziabher M, Lee H, Brothers RL, Allmendinger T, Vogt S, Costello P, Schoepf UJ (2009) Coronary CT angiography: automatic cardiac-phase selection for image reconstruction. *Eur Radiol* 19(8):1906–1913
- Goo HW (2011) Individualized volume CT dose index determined by cross-sectional area and mean density of the body to achieve uniform image noise of contrast-enhanced pediatric chest CT obtained at variable kV levels and with combined tube current modulation. *Pediatr Radiol* 41(7):839–847
- Goo HW (2012) CT radiation dose optimization and estimation: an update for radiologists. *Korean J Radiol* 13(1):1–11
- Goo HW (2013) Current trends in cardiac CT in children. *Acta Radiol* 54(9):1055–1062
- Goo HW, Yang DH, Hong SJ, Yu J, Kim BJ, Seo JB, Chae EJ, Lee J, Krauss B (2010) Xenon ventilation CT using dual-source and dual-energy technique in children with bronchiolitis obliterans: correlation of xenon and CT density values with pulmonary function test results. *Pediatr Radiol* 40(9):1490–1497
- Codella NC, Weinsaft JW, Cham MD, Janik M, Prince MR, Wang Y (2008) Left ventricle: automated segmentation by using myocardial effusion threshold reduction and intravoxel computation at MR imaging. *Radiology* 248(3):1004–1012
- Chuang ML, Gona P, Hautvast GL, Salton CJ, Blease SJ, Yeon SB, Breeuwer M, O'Donnell CJ, Manning WJ (2012) Correlation of trabeculae and papillary muscles with clinical and cardiac characteristics and impact on CMR measures of LV anatomy and function. *JACC Cardiovasc Imaging* 5(11):1115–1123
- Miller CA, Jordan P, Borg A, Argyle R, Clark D, Pearce K, Schmitt M (2013) Quantification of left ventricular indices from SSFP cine imaging: impact of real-world variability in analysis methodology and utility of geometric modeling. *J Magn Reson Imaging* 37(5):1213–1222
- Freling HG, van Wijk K, Jaspers K, Pieper PG, Vermeulen KM, van Swieten JM, Willems TP (2013) Impact of right ventricular endocardial trabeculae on volumes and function assessed by CMR in patients with tetralogy of Fallot. *Int J Cardiovasc Imaging* 29(3):625–631
- Walsh R, Salem Y, Shah A, Lai WW, Nielsen JC (2011) Repeatability of cardiac-MRI-measured right ventricular size and function in congenital heart disease. *Pediatr Radiol* 41(8):1000–1007
- Beerbaum P, Barth P, Kropf S, Sarikouch S, Kelter-Klopping A, Franke D, Gutberlet M, Kuehne T (2009) Cardiac function by MRI in congenital heart disease: impact of consensus training on interinstitutional variance. *J Magn Reson Imaging* 30(5):956–966

20. Sugeng L, Mor-Avi V, Weinert L, Niel J, Ebner C, Steringer-Mascherbauer R, Bartolles R, Baumann R, Schummers G, Lang RM, Nesser HJ (2010) Multimodality comparison of quantitative volumetric analysis of the right ventricle. *JACC Cardiovasc Imaging* 3(1):10–18
21. Mahnken AH, Bruder H, Suess C, Muhlenbruch G, Bruners P, Hohl C, Guenther RW, Wildberger JE (2007) Dual-source computed tomography for assessing cardiac function: a phantom study. *Invest Radiol* 42(7):491–498
22. Groen JM, van der Vleuten PA, Greuter MJ, Zijlstra F, Oudkerk M (2009) Comparison of MRI, 64-slice MDCT and DSCT in assessing functional cardiac parameters of a moving heart phantom. *Eur Radiol* 19(3):577–583
23. Koch K, Oellig F, Oberholzer K, Bender P, Kunz P, Mildenerger P, Hake U, Kreitner KF, Thelen M (2005) Assessment of right ventricular function by 16-detector-row CT: comparison with magnetic resonance imaging. *Eur Radiol* 15(2):312–318
24. Codella NC, Lee HY, Fieno DS, Chen DW, Hurtado-Rua S, Kochar M, Finn JP, Judd R, Goyal P, Schenendorf J, Cham MD, Devereux RB, Prince M, Wang Y, Weinsaft JW (2012) Improved left ventricular mass quantification with partial voxel interpolation: in vivo and necropsy validation of a novel cardiac MRI segmentation algorithm. *Circ Cardiovasc Imaging* 5(1):137–146
25. Kim HJ, Goo HW, Park SH, Yun TJ (2013) Left ventricle volume measured by cardiac CT in an infant with a small left ventricle: a new and accurate method in determining uni- or biventricular repair. *Pediatr Radiol* 43(2):243–246
26. Park EA, Lee W, Kim HK, Chung JW (2015) Effect of papillary muscles and trabeculae on left ventricular measurement using cardiovascular magnetic resonance imaging in patients with hypertrophic cardiomyopathy. *Korean J Radiol* 16(1):4–12
27. Goo HW, Park IS (2007) Left ventricular noncompaction in an infant: use of non-ECG-gated cardiac CT. *Pediatr Radiol* 37(2): 217–220